33. ORGANIC MATTER ALONG THE SEDIMENTARY SEQUENCES OF THE MOROCCAN CONTINENTAL MARGIN, LEG 79, SITES 545 AND 547[1]

Bernd R.T. Simoneit, College of Oceanography, Oregon State University
Vassil T. Vuchev, Kansas Geological Survey, University of Kansas
and
Joan O. Grimalt, College of Oceanography, Oregon State University[2]

ABSTRACT

The lipids and kerogens of 15 sediment samples from Site 547 (ranging from Pleistocene to Early Jurassic/Triassic) and 4 from Site 545 (Cretaceous) have been analyzed. A strong terrestrial contribution of organic matter was found, and significant autochthonous inputs were also present, especially at Site 545. Both strongly reduced and highly oxidized sediments have been found in the Cenozoic and Jurassic samples of Site 547. On the contrary, all the Cretaceous sections of Sites 547 and 545 are anoxic. Sediments from anoxic paleoenvironments are immature and have a high content of sterenes, diasterenes, steradienes, hopenes, and $\beta\beta$ hopanes. Samples from oxic paleoenvironments are mainly mature and their content of hopenes and steriod structures is below the detection level. Nevertheless, their hopane distributions have the immature $\beta\beta$ homologs as the predominant molecular markers. For Site 545 the most abundant molecular markers are ring A monoaromatic steranes, and their presence is attributed to microbial and chemical transformations during early diagenesis.

INTRODUCTION

Leg 79 is of interest from many geological aspects and particularly from an organic geochemical point of view. The eastern Atlantic has turned out to be one of the segments of the world ocean studied most during the entire history of deep sea drilling. A diverse and thick sequence of sediments was cored, ranging in age from Jurassic to Pleistocene and deposited in various and changing environments, interrupted by distinctive hiatuses overlapping or interspersed with block faulting of crystalline basement and diapiric salt movement. Such a sequence provides a unique opportunity for organic geochemical studies. The drilling results summarized initially (Hinz et al., 1982) and described in detail (site chapters, this volume) have provided such samples. Of particular interest is Site 547, which was drilled with reentry capability through the thickest sedimentary column (1030 m) and would probably have almost reached crystalline basement. This chapter is based primarily on data for specially selected samples from Site 547 with additional samples from Site 545 (the second deepest) taken for the Organic Geochemistry Panel. All possible on-board measurements were performed on the Site 547 samples during the cruise.

The goals of this study are to consider this thick sedimentary sequence in terms of general organic geochemistry. Three organic-rich facies are present within this sequence that require special attention, namely, Eocene claystones and chalks, Middle Cretaceous claystones, and Early Jurassic claystones and calcarenites. This variety of facies was deposited in a passive marginal basin, which has undergone a long and interruptive geological evolution starting with salt and red bed deposition in the Early Jurassic or Triassic and giving way to a hemipelagic and a pelagic deposition during the Late Jurassic through Cenozoic.

The analytical approach considers the content, types, sources, and maturity of the bulk organic matter, that is, the kerogen; the sources, diagenetic, and catagenetic changes of the extractable organic matter, that is the bitumen; and the overall petroleum potential of the sedimentary formations.

EXPERIMENTAL

Materials

The core samples studied here were taken from both holes at Site 547 and from Site 545. Site 547 is located in slope sediments of the structural high seaward of the regional Mazagan Slope (Fig. 1). The water depth at this site is 3940.5 m. Site 545 is located near the foot of the Mazagan Escarpment and is closest to the carbonate platform. At this location there is a major hiatus between the Mesozoic and Cenozoic, with the Cenomanian sequence covered by about 250 m of Pleistocene to Neogene chalks and oozes. The water depth is 3150 m.

All major units of the section were sampled at Site 547, including the three organic-rich intervals (Fig. 2, Table 1). Four samples at Site 545 are from the Middle Cretaceous claystones (Unit III), enriched in organic matter. All samples are considered to be geologically representative for the corresponding confidence limits (Fig. 2). Several exceptions, mainly with respect to carbonate content, are observed for the samples at Site 547, but they are within the confidence intervals.

Three analyses were carried out on samples from very close intervals of Section 547B-20-1 to elucidate the lithologic diversity of the Lower Jurassic sediments.

Lipids

The samples were freeze dried and then exhaustively extracted with chloroform and methanol (1:1) in a Soxhlet apparatus. The extracts were concentrated on a rotary evaporator and treated with BF_3 in methanol to derivatize free fatty acids. The extracts were then subject-

[1] Hinz, K., Winterer, E. L., et al., *Init Repts. DSDP*, 79: Washington (U.S. Govt. Printing Office).

[2] Addresses: (Simoneit) College of Oceanography, Oregon State University, Corvallis, OR 97331; (Vuchev, permanent address) Geological Institute, Bulgarian Academy of Science, 1113 Sofia, Bulgaria; (Grimalt permanent address) Instituto de Quimica Bio-organica, C.S.I.C., Jorge Girona Salgado, Barcelona 34, Spain.

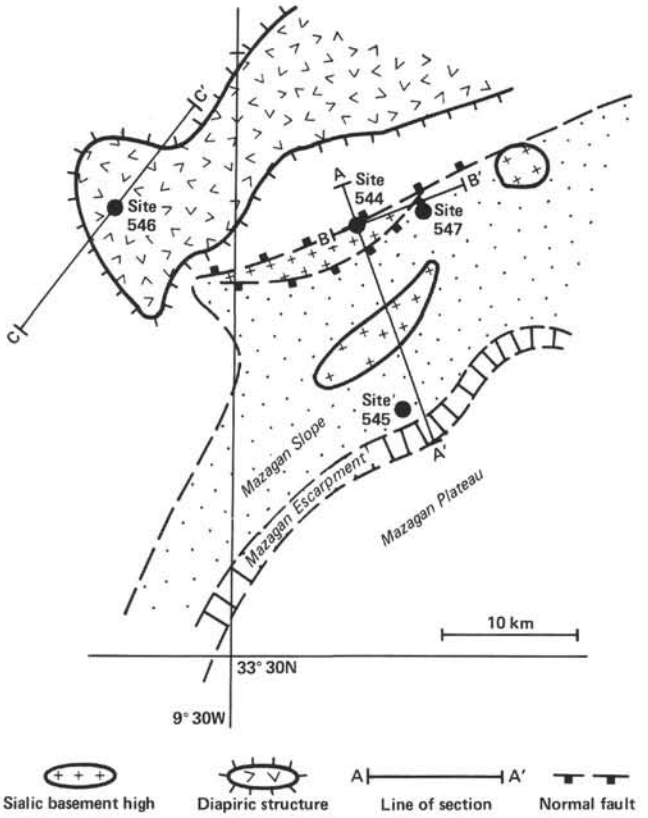

Figure 1. Mazagan Escarpment area, showing the location of Leg 79 Sites 545 and 547.

ed to thin-layer chromatography (TLC) on silica gel; hexane and diethyl ether (9:1) were used for eluent. The bands (after development with iodine vapor) corresponding to hydrocarbons, esters, and ketones were scraped off the TLC plates and eluted with methylene chloride. The hydrocarbon and some ester and ketone fractions were analyzed by gas chromatography (GC) and gas chromatography/mass spectrometry (GC/MS).

The GC analyses were carried out on a Varian Vista 44 gas chromatography system using a 25 m × 0.20 mm fused silica capillary column coated with DB-5 and programed from 40 to 280°C at 4°C per min.; He was the carrier gas.

The GC/MS analyses were performed on a Finnigan 4021 quadrupole mass spectrometer interfaced directly to a Finnigan 9610 gas chromatograph, equipped with a 30 m × 0.25 mm fused silica capillary column coated with SE-54. The GC conditions for the GC/MS analyses were the same as those employed in the analytical GC system. The mass spectrometric data were acquired and processed with a Finnigan-Incos 2300 data system.

Bulk Organic Matter

The measurements of $CaCO_3$, C_{org}, and N_{org} shown in Figure 2 and associated with the samples taken for the Organic Geochemistry Advisory Panel (OGP) were carried out on small amounts taken from just below and above the 30-cm sections of the bulk samples. All colors including those of the bitumens were determined conventionally following the Rock–Color Chart of the Geological Society of America.

The Hewlett-Packard CHN-Analyzer was utilized on-board and it worked perfectly with samples of 20 mg. Rock-Eval pyrolysis analyses were carried out on board with the Girdel instrument. The sample, weights were kept around 100 mg, but smaller amounts of about 25–30 mg were found adequate when richer sediments were pyrolyzed. The Rock-Eval instrument is designed to measure hydrocarbon potential and maturity of source rock samples, based on the selective detection and quantitation of hydrocarbons and CO_2 by programmed pyrolysis (Espitalié et al., 1977; Roucaché et al., 1979). Several parameters are obtained by this technique (Peters and Simoneit, 1982). The free hydrocarbons (bitumen) are thermally distilled from the sample and the quantity (mg HC/g sample) determined by a flame ionization detector represents the first peak (S1). The second peak (S2) comprises the hydrocarbons generated by pyrolytic degradation of the remaining organic matter (kerogen) (mg HC/g sample). The carbon dioxide generated from organic matter is separated and analyzed as a third peak (S3) (mg CO_2/g sample) using a thermal conductivity detector. The temperature of maximum hydrocarbon yield (T_{max}) is also monitored. The hydrogen index (HI) corresponds to the amount of hydrocarbons (S2) normalized to the total organic carbon (TOC) content of the sample (mg HC/g C_{org}). The oxygen index (OI) corresponds to the amount of CO_2 (S3) normalized to TOC (mg CO_2/g C_{org}). The HI and OI correlate well with atomic H/C and O/C, respectively (Espitalié et al., 1977).

RESULTS AND DISCUSSION

Lithological and Organic Matter Measurements

A few comments should be added to the basic results of the contents and distributions of $CaCO_3$ and C_{org} along the sedimentary section studied. The data are shown in Figure 2 for Sites 547 and 545, discussed in further detail in the corresponding site chapters (this volume), and listed in Table 1. There are two major subdivisions of this section: (1) medium and highly calcareous, uniform oozes in the Cenozoic with a low C_{org} content; (2) low and medium to highly calcareous sediments in the Mesozoic, with a gradually increasing and then decreasing carbonate content versus depth, and a moderate to low C_{org} content, which reaches a maximum in the middle Cretaceous nanno-bearing chalks.

Each subdivision has an interval anomalously rich in C_{org}. Unit III of Hole 547A is late Eocene in age and consists mainly of a matrix with claystones and chalks, containing clasts and conglomerate beds of similar sediments. Samples 547A-18-1, 57–73 cm and 547A-20-4, 120–125 cm are from this unit, and they are among the richest in organic carbon content of the whole sequence. R. Mark Leckie carried out a quantitative examination of Sample 547A-18-1, 57–73 cm with respect to the composition and contents of foraminifers and found that among a total of 435 tests there were 227 (52.2%) planktonic and 208 (47.8%) calcareous benthic specimens. All were well preserved with many juvenile forms, especially among the planktonic species. The assemblage appears to have a minimal component from recycling, though Sample 547A-18-1, 57–73 cm is itself part of the clast of middle Eocene age. Resedimentation is considered responsible for the clasts and debris flows of the entire unit (Site Chapter, this volume).

The lowest part of Subunit VIB (891–924 m) of Hole 547B is from the Mesozoic subdivision. It is Early Jurassic in age and contains several layers of organic-rich claystones and calcarenites among a lithologically diverse and disturbed sequence. Some layers appear very "coaly" and shaley, although claystones within the unit contain well-preserved benthic foraminifers.

There are a few significant correlations between the noncarbonate material and C_{org} for both Sites 547 and 545 (Site Chapters, this volume). At Site 547 Units I, IIA, IVA, and IVB, VB, and VII show positive correlations. These are sequences with presumed uniform sedimentation, where the sediment and organic matter accumulations can be related to similar factors. This is not

the case for the two organic-rich intervals in the late Eocene and Early Jurassic discussed previously. The same kind of correlation was found for all Cenozoic units at Site 545, again marking the intervals of stable sedimentation.

The contents and distribution of N_{org} for all units and samples studied (Table 1) parallel those of C_{org}. The ratios of C_{org} to N_{org} for the organic-rich Jurassic samples were anomalously high, which may indicate a contribution of terrestrially derived organic matter the sediments. This may also be the case for the Eocene samples that are enriched in C_{org}. The terrestrial influx of organic detritus is, however, not indicated by the Rock-Eval data and the high C/N ratio may thus reflect increased maturity or degradation of the organic matter (e.g., Simoneit, 1982).

Extractable Organic Matter (bitumen)

Good yields and percentages of extractable bitumen were obtained with few exceptions, namely, from Samples 547A-4-1, 110–116 cm and 547A-10-2, 120–136 cm. Varicolored claystone and mudstone comparatively poor in C_{org} from the lowest part of the section at Site 547 also contained a significant amount of bitumen. There is one remarkable feature of the extract data: the bituminosity of the organic matter (beta) is low and indicates the syngenetic character of the extractable organic constituents in the samples (Table 2). The bituminosity or bitumen extraction ratio has been used to estimate organic matter transformation (maturation) and to diagnose bitumen migration (i.e., allochthonous bitumen content) (Vuchev, 1974). The colors of the bitumens, although dissolved in CH_2C1_2, match, at least partly, the colors of the corresponding sediments (Tables 1 and 2).

Hydrocarbons

The GC traces of most of the hydrocarbon fractions are shown in Figures 3 and 4. The resolved components consist primarily of *n*-alkanes and cyclic molecular markers (sterenes and triterpenes), and various envelopes of the unresolvable branched and cyclic compounds are also evident. Such chromatograms have been described earlier from other drill sites in the Cretaceous of the eastern Atlantic (e.g., Rullkötter et al., 1982). The distribution diagrams of the *n*-alkanes are shown in Figure 5 to clarify their distribution patterns and ranges in some of these complex mixtures.

The *n*-alkanes of all samples have a dominant contribution from terrestrial plant waxes (Simoneit, 1978). The odd carbon number alkanes $>C_{24}$ are most abundant in all samples, except for the Eocene example (Section 547A-18-1) where the maximum around C_{21} is present at an equivalent concentration. These allochthonous terrigenous hydrocarbons exhibit different carbon-number maxima, depending on their geologic age and the location of the drill site. Thus, all samples examined from Site 545 have a maximum of n-C_{25} and those from Site 547 have maxima at n-C_{31} (Pleistocene to late Eocene and Jurassic) or at n-C_{27} (late Eocene to late Albian). This aspect is emphasized further by the ratio of $(n\text{-}C_{29} + n\text{-}C_{31})/(n\text{-}C_{25} + n\text{-}C_{27})$ given in Table 2. Values greater than about 1.3 reflect the higher carbon number maxima and those less than 1.3 indicate lower ones. The plant wax signatures with a maximum at n-C_{31} may reflect a source from grassland or swamp vegetation and those with a maximum at n-C_{27} may be derived from marsh or sea grasses (Simoneit and Mazurek, 1979b). In fact, the *n*-alkane patterns in the core sections from Site 547 parallel those from Site 397 further to the south, where the Pleistocene samples exhibit a maximum at n-C_{31} and the Cretaceous samples at n-C_{27} (cf. Figs. 5R and S, Simoneit and Mazurek, 1979b). The maximum at n-C_{29} for Section 547B-4-2 in the late Albian (Fig. 5H) has also been observed for a claystone of the same age from Site 398 at the Vigo Seamount (Simoneit and Mazurek, 1979a). The n-C_{31} predominance for the Jurassic samples from Site 547 was also observed in the same geologic age sequence at Site 391 in the Blake-Bahama Basin (cf. Fig. 5T; Stuermer and Simoneit, 1978).

Autochthonous marine hydrocarbons are more evident at Site 545 where the *n*-alkanes exhibit a maximum at C_{17} with no carbon number preference from C_{14} to C_{20}, which is indicative of an algal source. At Site 547, the hydrocarbons from Sections 547A-18-1 and 547A-63-3 only exhibit a microbial autochthonous component.

The concentrations of pristane (Pr) and phytane (Ph) can be correlated with the degree of anoxicity during sedimentation and subsequent diagenesis (Didyk et al., 1978). In very oxidized sediments (cf. HI and OI correlation of the kerogens below) there is a tendency towards a higher content of pristane than phytane (Pr/Ph <1, Table 2) and their overall concentrations are low (Fig. 5). Sections 547A-4-1, 547A-10-2, 547A-41-1, 547B-20-1, and 547B-26-1 reflect oxic sedimentary conditions. Furthermore, it should be noted that the quantities of these isoprenoid hydrocarbons are so low in some cases that the Pr/Ph may be subject to some degree of uncertainty due to the analytical constraints. However, in the case of high isoprenoid concentrations (anoxic sedimentary environment) this is a clearly not a problem. In this respect there are three coincident parameters that define the oxic sections of Site 547 mentioned previously: (1) a low content of organic carbon ($<1\%$, carbonate-free); (2) the kerogen (discussed later) has a high oxygen index and low hydrogen index; and (3) a low content of isoprenoid hydrocarbons ($Pr + Ph/n\text{-}alk_{max} < 0.2$) with Pr/Ph > 1. The anoxic sediments are characterized by their enhanced organic matter contents, high phytane concentrations, and hydrogen-rich kerogen.

The total concentrations of *n*-alkanes in these samples are related to their overall organic matter contents and to the environmental conditions during their sedimentation. The lean and oxic sections have *n*-alkane concentrations in the range of 250–500 ng/g of dry sediment and the more anoxic and organic-rich samples range up to 1400 ng/g. Considering the *n*-alkane concentration versus organic carbon content (Table 2), it is obvious that some of the organic-rich sediments have anomalously low amounts of hydrocarbons (e.g., Sections 547A-18-1, 547A-20-4 and 547B-20-1). In these cases, the strong an-

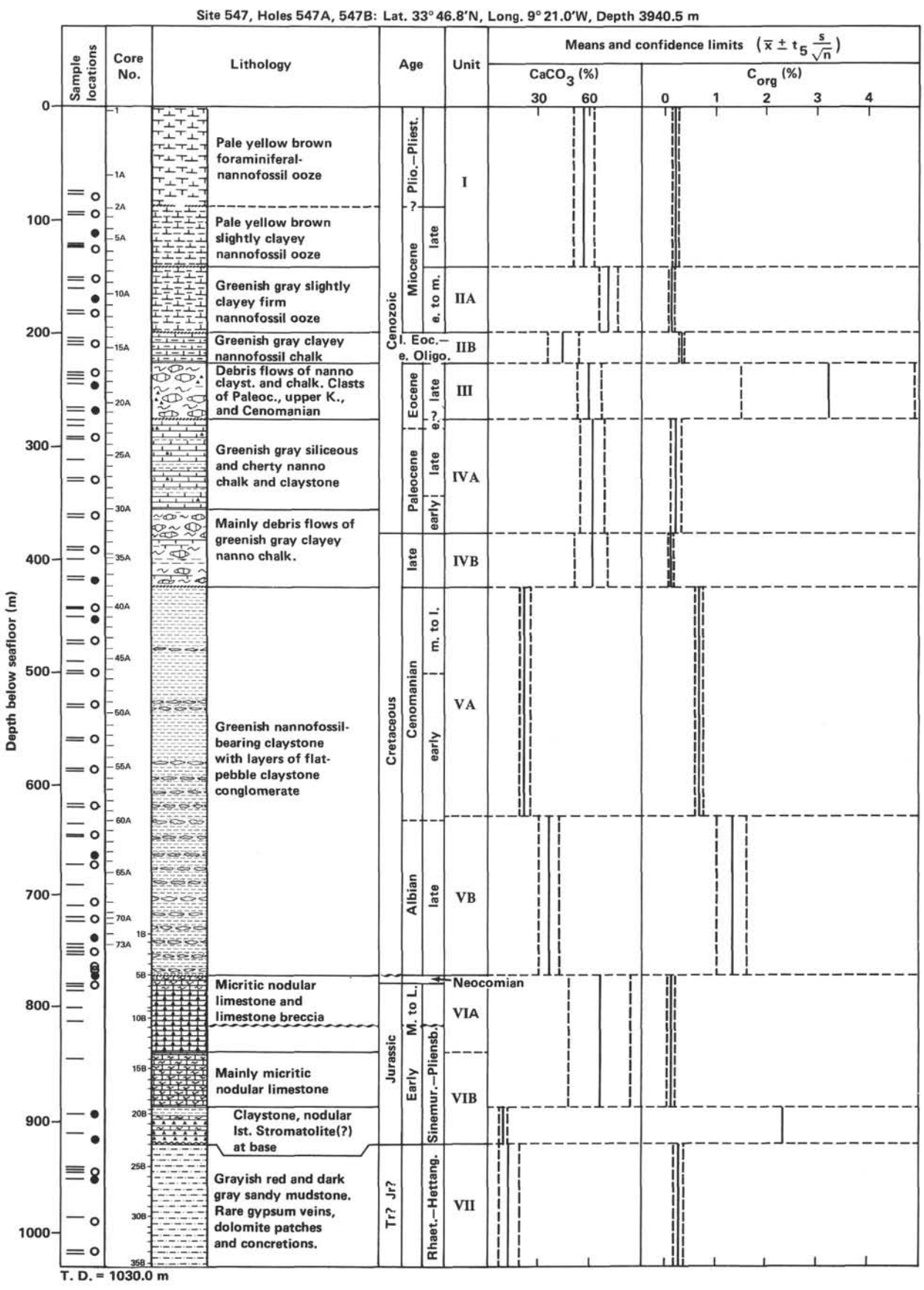

Figure 2. Sediment lithology, ages, mean concentrations of organic and carbonate carbon for sedimentary units, and locations of samples taken from this study.

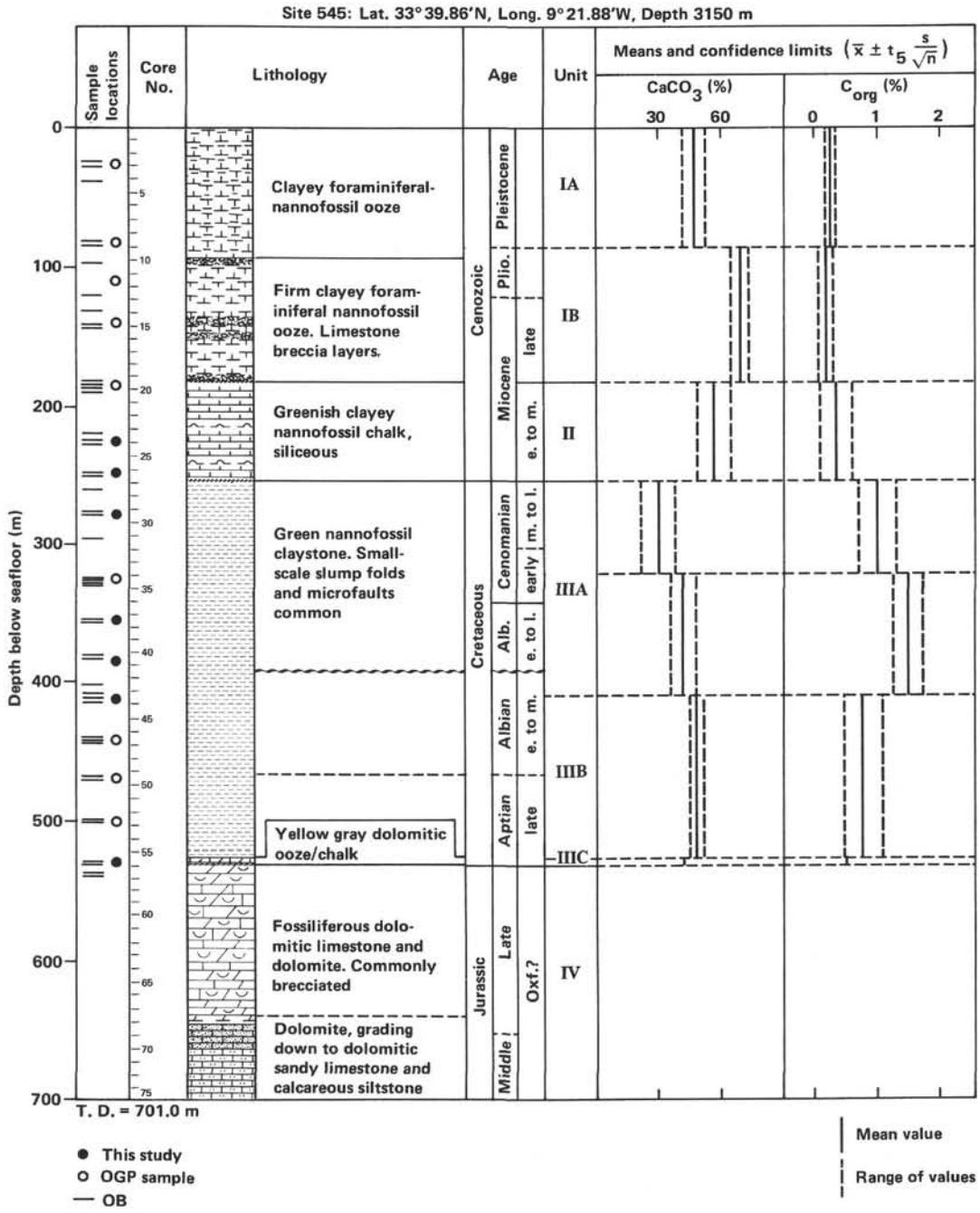

Figure 2. (Continued).

oxic environmental conditions have perhaps preserved a significant fraction of the lipids as more polar components (e.g., fatty acids, alcohols, ketones, etc.) so that the hydrocarbons constitute a relatively minor fraction of the total.

The unresolved complex mixture (UCM, hump) of branched and cyclic hydrocarbons of the many samples from Site 547 are bimodal (Fig. 3), with maxima at about C_{20} or C_{21} and at C_{29} or C_{30}. Since all these samples are relatively immature, the UCM at lower retention time is attributable to a marine origin and the other one may be derived from diagenesis of heavier, mostly terrestrial lipid residues. Only Section 547B-26-1 exhibits a unimodal hump, maximizing at about C_{25}. It is the oldest section sampled and may reflect the effects of a higher geothermal gradient that caused the onset of bitumen generation from kerogen. A large amount of UCM is present in the samples from Site 545 and maximizes around the retention time of *n*-C_{17} (Fig. 4). The relatively low concentration of *n*-alkanes $< C_{20}$ may indicate a strong influence of hydrocarbon degradative microorganisms active during sedimentation. This phenomenon is common

Table 1. Carbonate, C_{org}, and N_{org} contents of samples from Sites 547 and 545.

Sample (interval in cm)	Sub-bottom depth (m)	Unit/ Subunit	Age	Lithology	$CaCO_3$ (%)	C_{org} (%)		N_{org} (%)		$\frac{C_{org}}{N_{org}}$
						Noncarbonate residue	Total sediment	Noncarbonate residue	Total sediment	
Hole 547A										
4-1, 110-116	99.5	I	Pliocene	Nanno ooze, clayey, pinkish gray	80.4	0.38	0.07	0.09	0.02	4.2
10-2, 120-136	158.2	IIA	middle Miocene	Nanno ooze, clayey, bluish white	73.3	0.73	0.19	0.10	0.03	7.3
18-1, 57-73	232.1	III	late Eocene	Nanno chalk, clayey, slightly silty, light olive gray	68.2	17.15	5.45	0.79	0.25	21.7
20-4, 120-125	256.2	III	late Eocene	Nanno chalk, clayey, slightly silty, light olive gray	57.5	7.19	3.06	0.27	0.11	26.6
41-1, 34-50	440.9	VA	late Cenomanian	Claystone, light olive gray, nanno-bearing	15.7	0.57	0.48	0.06	0.05	9.5
63-3, 110-128	653.6	VB	late Albian	Nanno chalk, clayey, light olive gray	32.5	1.38	0.93	0.10	0.07	13.8
72-2, 24-40	726.4	VB	late Albian	Nanno chalk, clayey, slightly silty, light olive gray	58.0	1.86	0.78	0.12	0.05	15.5
Hole 547B										
4-2, 110-126	755.7	VB	late Albian	Nanno chalk, clayey, slightly silty, light olive gray	38.5	1.89	1.16	0.12	0.07	15.8
4-3, 85-101	757.1	VB	late Albian	Nanno chalk, clayey, slightly silty, light olive gray	48.8	1.39	0.71	0.10	0.05	13.9
4-5, 10-26	759.5	VB	late Albian	Nanno chalk, clayey, slightly silty, light olive gray	41.1	1.50	0.88	0.11	0.06	13.6
20-1, 13-14(I)	891.1	VIB	Early Jurassic	Claystone, olive gray	9.5	7.47	6.76	0.16	0.14	46.7
20-1, 5-23(II)	891.1	VIB	Early Jurassic	Calcarenite, greenish gray, slightly silty	63.4	5.51	2.02	0.15	0.05	36.7
20-1, 5-23(III)	891.1	VIB	Early Jurassic	Claystone, dark greenish gray, waxy	12.9	10.21	8.89	0.18	0.16	56.7
22-2, 36-55	907.0	VIB	Early Jurassic	Calcareous claystone, light olive gray	28.4	0.66	0.44	0.06	0.04	11.0
26-1, 20-36	941.7	VII	Early Jurassic/ late Triassic	Calcareous mudstone, silty, grayish olive	34.2	0.42	0.28	0.05	0.03	8.4
Hole 545										
29-1, 145-150	266.9	IIIA	late Cenomanian	Nannofossil claystone, green	33.6	1.52	1.01	0.11	0.07	13.8
37-2, 145-150	343.9	IIIB	late Albian	Nanno chalk, clayey, green	50.8	1.49	0.73	0.10	0.05	14.9
43-4, 145-150	403.9	IIIB	middle Albian	Nanno chalk, clayey, silty, green	41.3	2.90	1.70	0.16	0.09	18.1
55-5, 120-123	519.2	IIIC	late Aptian	Nanno chalk, clayey, silty, green	53.6	2.07	0.96	0.10	0.05	20.7

in recent sediments with some degree of anoxicity and a high rate of hydrocarbon accumulation (Wakeham and Carpenter, 1976; Reed, 1977), and usually the shorter chain hydrocarbons are degraded first (Giger et al., 1980).

Molecular Indicators

The dominant molecular markers found in the hydrocarbon fractions are steroid and triterpenoid derivatives and they are summarized in Table 3. The salient features

Table 2. Bitumen in sediments from Sites 547 and 545.

Core-section	C_{org} in total sediment (dry wt.%)	g	Yield: Dry wt.% of sediment	Yield: mg/g C_{org}	Bitumen (extractable) color (GSA, rock-color chart)	Bituminosity beta = bitumen / C_{org}	Hydrocarbons (*n*-alkanes): yield (ng/g)[a]	Hydrocarbons (*n*-alkanes): CPI[b]	Hydrocarbons (*n*-alkanes): C_{max}[c]	Pr/Ph[d]	$\frac{n\text{-}C_{29} + n\text{-}C_{31}}{n\text{-}C_{25} + n\text{-}C_{27}}$
Hole 547A											
4-1	0.07	0.0022	0.004	63	Grayish yellow (5Y 8/4)	6.3	250 (660)	3.2	29,31	0.63	2.34
10-2	0.19	0.0028	0.006	32	Light olive brown (5Y 5/6)	3.2	360 (490)	3.3	29,31	1.00	2.43
18-1	5.45	0.1000	0.242	44	Grayish olive green (5GY 3/2)	4.4	1200 (70)	2.4	21,29,31	0.44	1.33
20-4	3.06	0.0576	0.113	37	Grayish olive green (5GY 3/2)	3.7	830 (110)	2.0	25,27,31	0.59	0.82
41-1	0.48	0.0113	0.020	42	Moderate brown (5YR 3/4)	4.2	510 (890)	2.4	25,27,29	1.25	0.83
63-3	0.93	0.0454	0.073	78	Dusky brown (5YR 2/2)	7.8	950 (690)	2.1	Ph,23,25,27	0.68	0.69
72-2	0.78	0.0539	0.073	94	Dusky brown (5YR 2/2)	9.4	770 (410)	1.8	25,27,31	0.30	0.78
Hole 547B											
4-2	1.16	0.0751	0.110	95	Dusky brown (5YR 2/2)	9.5	1180 (620)	2.5	Ph,25,27,31	0.53	1.34
4-3	0.71	0.0653	0.098	138	Dusky brown (5YR 2/2)	13.8	750 (540)	2.6	25,27,31	0.45	0.74
4-5	0.88	0.0441	0.060	68	Dusky brown (5YR 2/2)	6.8	900 (600)	2.4	25,27,31	0.36	0.71
20-1	8.89	0.1249	0.169	19	Dusky brown (5YR 2/2)	1.9	1300 (240)	3.1	29,31	0.36	1.50
22-2	0.44	0.0084	0.011	25	Moderate brown (5YR 3/4)	2.5	460 (700)	3.2	Ph, 29, 31	0.50	1.76
26-1	0.28	0.0135	0.018	64	Moderate brown (5YR 3/4)	6.4	290 (690)	1.4	18,25	0.67	0.58
Hole 545											
29-1	1.01	0.0297	0.050	50	Dusky brown (5YR 2/2)	5.0	1050 (690)	2.0	25,27	1.30	0.69
37-2	0.73	0.0250	0.057	78	Dusky brown (5YR 2/2)	7.8	760 (510)	1.9	23,25,27	0.80	0.76
43-4	1.70	0.0501	0.103	61	Dusky brown (5YR 2/2)	6.1	1400 (480)	2.7	25,35	0.56	0.51
55-5	0.96	0.0238	0.042	44	Dusky brown (5YR 2/2)	4.4	950 (460)	2.2	17,25,31	1.07	0.92

[a] Hydrocarbon yield expressed as ng/g dry sediment and in parentheses as ng/g organic carbon.
[b] Carbon preference index is summed from C_{14} to C_{38}, odd-to-even ratio.
[c] Homologs with maximum concentration; dominant homolog is underscored.
[d] Pristane to phytane ratio (Didyk et al., 1978).

of typical mass chromatograms (m/z 191, 257, 215, 217, and 211) for these molecular indicators are shown for two examples in Figures 6 and 7.

The oxic samples (e.g. Sections 547A-4-1 and 547B-26-1) contain no detectable levels of steroid compounds and only traces of triterpenoids. No inferences can be drawn from the limited triterpane content of Section 547A-4-1 and those of the other sample are immature based on the stereomer distribution.

The samples coming from anoxic paleoenvironments contain major concentrations of triterpenoids and steroidal compounds (Table 3), in some cases exceeding the *n*-alkane concentrations. The late Eocene sample (Section 547A-18-1) contains mainly sterenes and various hopanoids. The sterenes are immature and are comprised of Δ^4 and Δ^5 - monounsaturated (I) and traces of $\Delta^{5,22}$ - diunsaturated C_{27} to C_{29} homologs, with some 5α(H)-steranes (II). The hopanoids are also immature and consist primarily of the 17β(H),21β(H)-series (III) ranging from C_{27} to C_{31} without C_{28} and various olefins. Isohop-13(18)-ene (IV) is the dominant triterpenoid, with lesser amounts of trisnorhop-17(21)-ene (V, R = H); hop-17(21)-ene (V, R = C_3H_7); fern-7-ene (VI, Δ^7); fern-8-ene (VI, Δ^8); and unknown C_{27} and C_{30} isomers. The late Albian samples (Sections 547A-72-2, 547B-4-2, 547B-4-3, and 547B-4-5, e.g., Fig. 6) contain predominantly sterenes and lesser amounts of hopanoids, also with stereochemistries indicative of immature organic matter. The sterenes are composed of Δ^4- and Δ^5-monounsaturated (I), diasterenes (VII), and 5α(H)-steranes (II) [$\gg$ 5β(H)-steranes], ranging from C_{27} to C_{29} with a predominance of C_{27} and significant amounts of the C_{29} homologs. Monoaromatic steranes (VIII) are present as minor components with a predominance of C_{27}. The triterpenoids consist of 17β(H)-hopanes (III) ranging from C_{27} to C_{31} without C_{28} and various olefins and unknown compounds. Isohop-13(18)-ene (IV); hop-17(21)-ene (V, R = C_3H_7); another isomer; and trisnorhop-17(21)-ene (V, R = H) are the major triterpenes present. Similar molecular marker distributions have been identified in

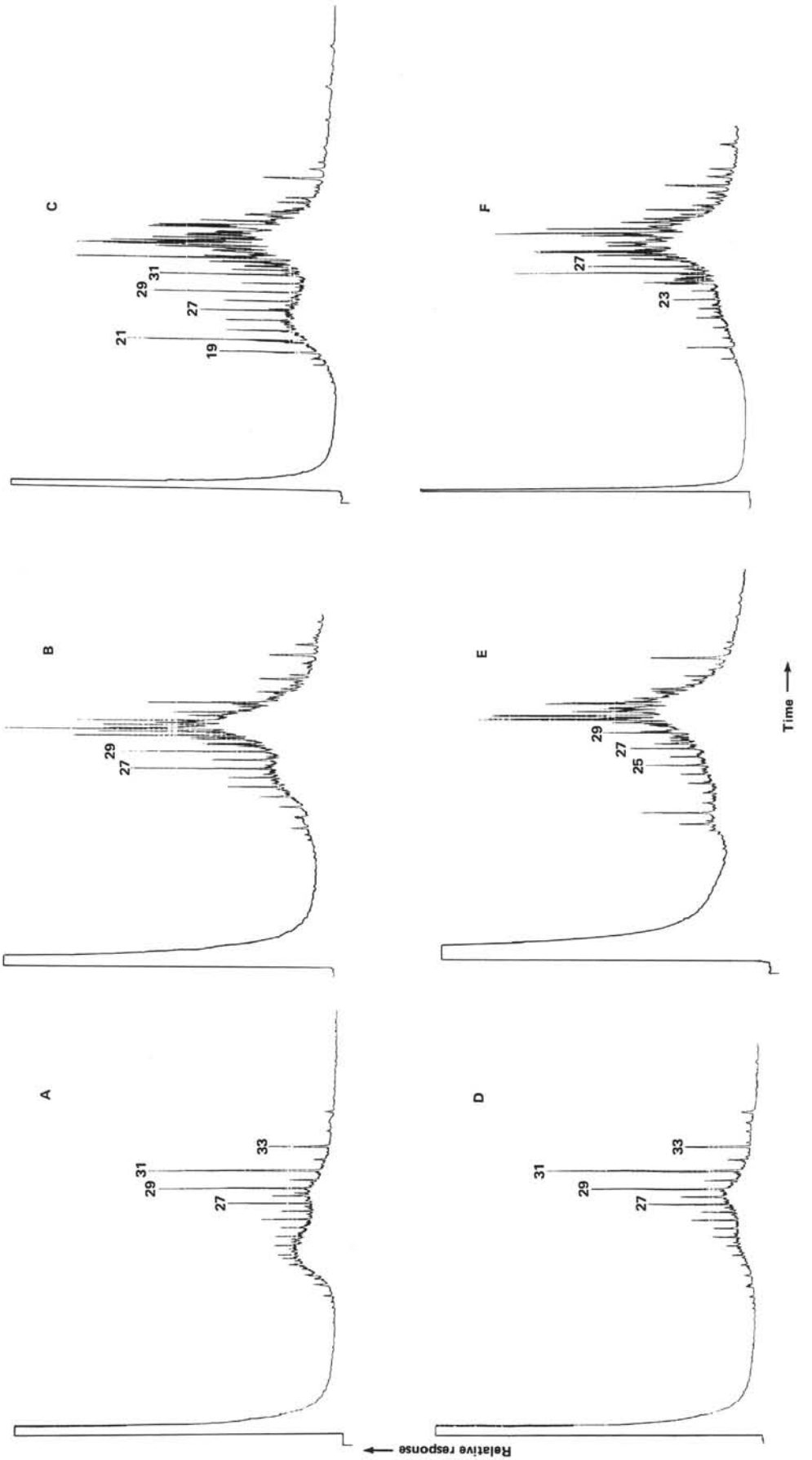
A
B
C
D
E
F
33
31
29
27
25
23
21
19
Relative response
Time

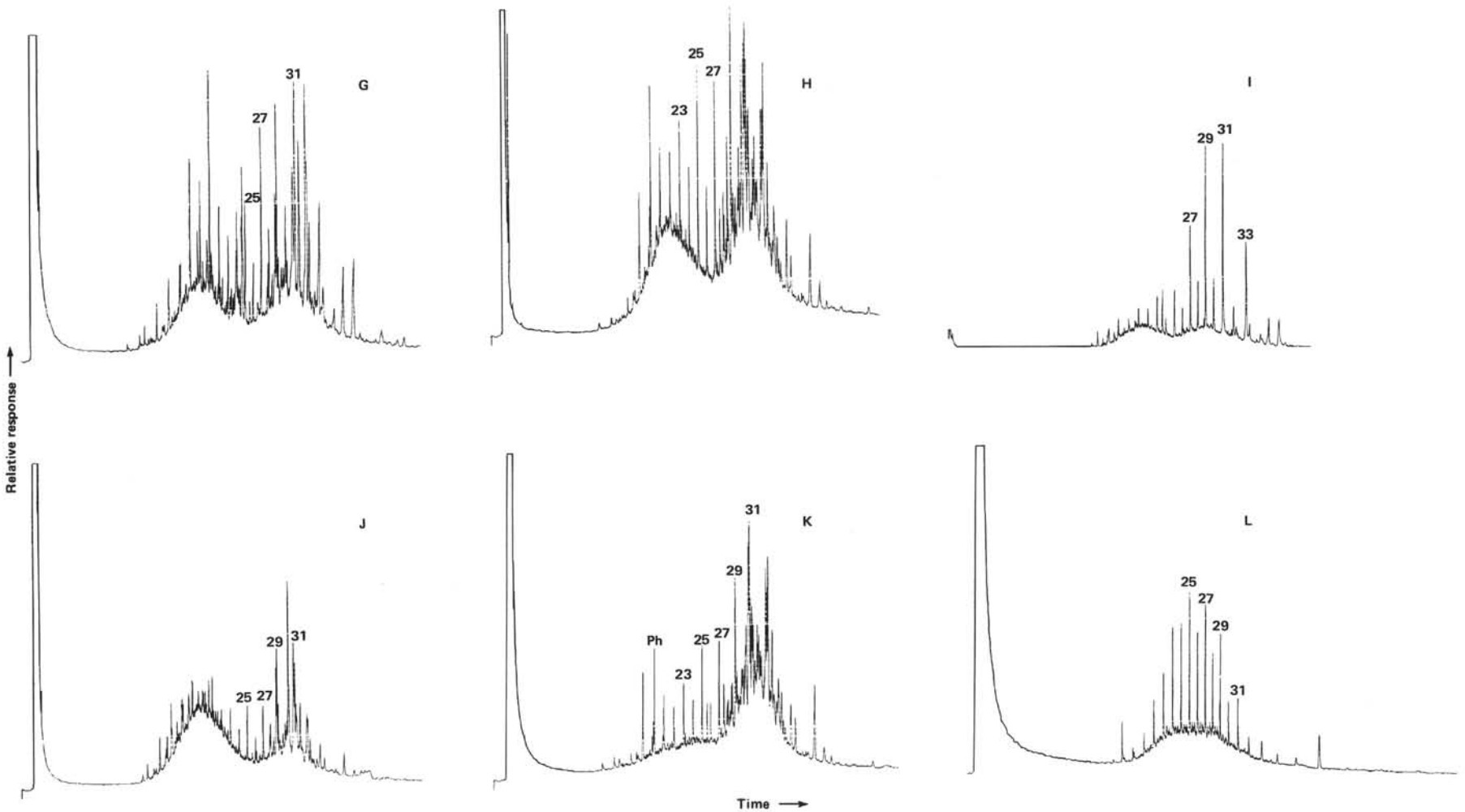

Figure 3. Capillary gas chromatograms (operating conditions are given in the text) of the hydrocarbon fractions from samples at Site 547 (arabic numerals indicate *n*-alkanes): A. 547A-4-1, 110–116 cm. B. 547A-10-2, 120–136 cm. C. 547A-18-1, 57–73 cm. D. 547A-20-4, 120–125 cm. E. 547A-41-1, 34–50 cm. F. 547A-63-3, 110–128 cm. G. 547A-72-2, 24–40 cm. H. 547B-4-3, 85–101 cm. I. 547B-4-5, 10–26 cm. J. 547B-20-1(II), 5–23 cm. K. 547B-22-2, 36–55 cm. L. 547B-26-1, 20–36 cm.

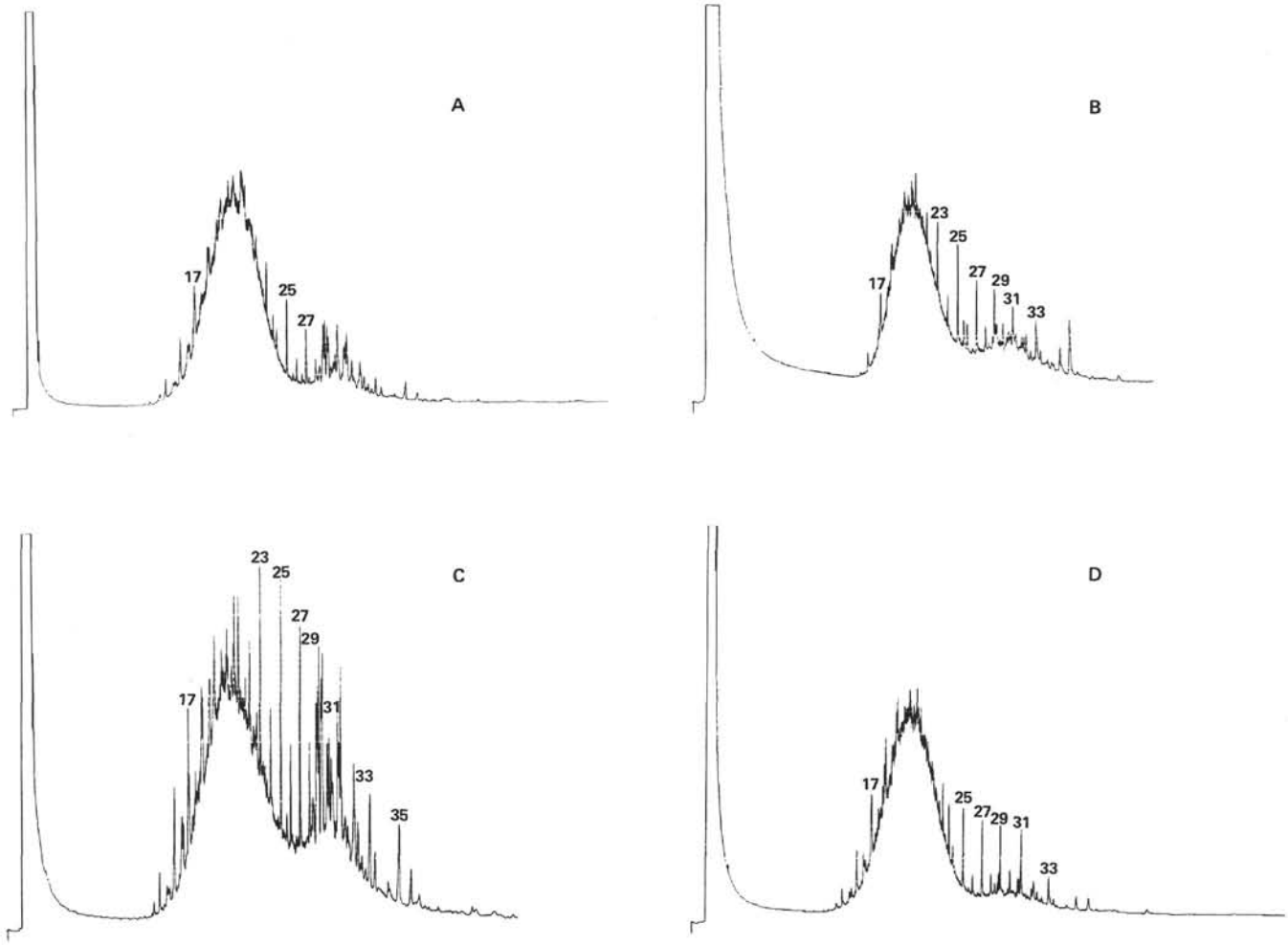

Figure 4. Capillary gas chromatograms of the hydrocarbon fractions from the samples at Site 545 (arabic numerals indicate *n*-alkanes): A. 545-29-1, 145–150 cm. B. 545-37-2, 145–150 cm. C. 545-43-4, 145–150 cm. D. 545-55-5, 120–123 cm.

other Cretaceous samples from the eastern Atlantic (e.g., Rullkötter et al., 1982). The Early Jurassic sample (Section 547A-20-1) also contains immature sterenes and triterpenoids. The dominant compounds are the triterpenes: isohop-13(18)-ene (IV), hop-17(21)-ene (V), and trisnorhop-17(21)-ene (V), with lesser amounts of the 17β(H)-hopane series (III) from C_{27} (no C_{28}) to C_{33} and traces of moretanes and 17α(H)-hopane. Monounsaturated sterenes (Δ^4 and Δ^5) and 5α(H)-steranes are present as minor components.

Three mid-Cretaceous samples from Site 545 contain predominantly immature and possibly oxidized steroid residues and lesser amounts of triterpenoids (Table 3). The major steroid residues for these samples are monoaromatic steranes (VIII), ranging from C_{27} to C_{29}, with a strong maximum at C_{29} and three different isomers at each carbon number (e.g., Fig. 7). The mass spectrometric fragmentation pattern of the dominant isomer (e.g., Fig. 7C) fits with that of an authentic standard described by Spyckerelle (1975) and Hussler et al. (1981). These compounds were also identified in other DSDP samples of Cretaceous age from the eastern North Atlantic (Hussler et al., 1981), but their origin could not be defined. We suggest that these compounds may represent an oxidized steroid component, and based on the maximum concentration at C_{29}, derived from terrestrial sources since other terrigenous lipids are also present. The Δ^4 and Δ^5-sterenes (I) are the next significant markers, ranging from C_{27} to C_{29}, with lesser concentrations of $\Delta^{5,22}$-diunsaturated sterenes, diasterenes (VII), and 5α(H)-steranes, in these cases with a predominance of C_{27}. The minor amounts of triterpenoids consist of the 17β(H)-hopanes, ranging from C_{27} to C_{33} (no C_{28}) (III), and some hop-17(21)-ene, isohop-13(18)-ene, fern-7-ene (VI), other isomers of olefins, 17α(H)-hopane, and moretane (e.g., Fig. 7).

Varying amounts of sesquiterpenoid and diterpenoid residues are found in the Jurassic and Cretaceous sections of both sites. The sesquiterpenoidal compounds are mainly cadalene (IX), with in some cases 5,6,7,8-tetrahydrocadalene, and they occur in the Cretaceous samples. The major diterpenoidal compounds are retene (X), dehydroabietin (XI), simonellite (XII), and 13-methylpodocarpa-8,11,13-triene (XIII). These compounds are indicative of a terrigenous origin, and the absence of the more reduced species (e.g., fichtelite, dehydroabietane) suggests some oxidative diagenesis during transport (Simoneit, 1977; in press).

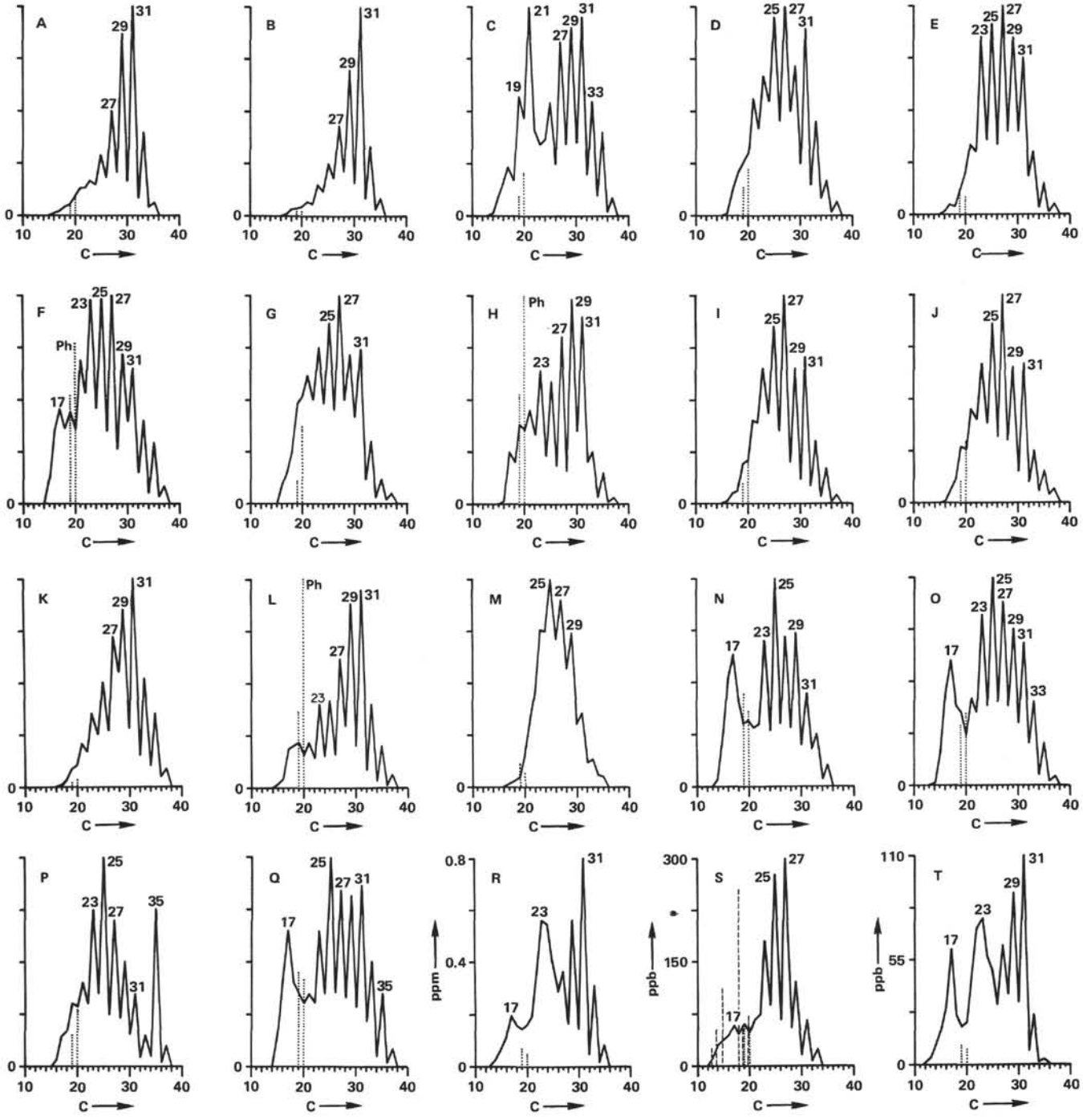

Figure 5. Distribution diagrams (concentration versus carbon number) of *n*-alkanes for all samples analyzed (... = isoprenoids): A. 547A-4-1, 110–116 cm. B. 547A-10-2, 120–136 cm. C. 547A-18-1, 57–73 cm. D. 547A-20-4, 120–125 cm. E. 547A-41-1, 34–50 cm. F. 547A-63-3, 110–128 cm. G. 547A-72-2, 24–40 cm. H. 547B-4-2, 110–126 cm. I. 547B-4-3, 85–101 cm. J. 547B-4-5, 10–26 cm. K. 547B-20-1(II), 5–23 cm. L. 547B-22-2, 36–55 cm. M. 547B-26-1, 20–36 cm. N. 545-29-1, 145–150 cm. O. 545-37-2, 145–150 cm. P. 545-43-4, 145–150 cm. Q. 545-55-5, 120–123 cm. R. 396-6-3, 120–135 cm (Simoneit and Mazurek, 1979b). S. 397A-51-4, 100–112 cm (Simoneit and Mazurek, 1979b). T. 391C-52-2, 3–10 cm (Stuermer and Simoneit, 1978).

The molecular markers of these samples are immature, even into the Jurassic. The oxidized samples contain very low levels of molecular markers and they are more mature than those of the anoxic sediments. The anoxic samples from the Cretaceous and Jurassic contain mainly steroid residues and triterpenoids whose carbon skeleton distributions indicate a mixed origin from principally marine, autochthonous and from lesser terrigenous, allochthonous sources. This is based primarily on the significant concentrations of the C_{29} steroid skeleton versus the C_{27} homolog (Huang and Meinschein, 1979) and possibly the monoaromatic steroid se-

Table 3. Molecular markers in sediments from Sites 547 and 545.

Core-section	Characteristics	Age	Main hopanoids[a]	Main steroids[a]	Main diterpenoids[a]	Aromatics	Others
Site 547							
4-1	Oxic	Pleistocene late Miocene	Very weak	Under detectable level	Not found		
18-1	Anoxic	late Eocene	Isohop-13(18)-ene Hop-17(21)-ene Trisnorisohop-13(18)-ene 17β,21β(H)-hopane 17β(H)-trisnorhopane 17β,21β(H)-norhopane 17β,21β(H)-homohopane 17α,21β(H)-hopane	5α,14α,17α(H)-cholestane Δ^4-sterenes $C_{29} > C_{27}$ Δ^5-sterenes $C_{29} > C_{27}$ A monoaromatic steranes C_{27} $\Delta^{5,22}$steradienes C_{28}	Not determined		
41-1	Oxic	late Cenomanian	Weak 17β,21β(H)-hopane 17β,21β(H)-homohopane	Diasterenes $C_{29} > C_{27}$	Dehydroabietane Dehydroabietin 19-norabieta-8,11,13-triene		
72-2	Anoxic	late Albian	17β(H)-trisnorhopane	Diasterenes $C_{27} > C_{29}$ 5α,14α,17α(H)-cholestane Δ^5-sterenes $C_{27} > C_{29}$ Δ^4-sterenes $C_{27} > C_{29}$ $\Delta^{5,22}$-steradienes C_{28}	Dehydroabietin 19-norabieta-8,11,13-triene 13-methylpodocarpa-8,11,13-triene 5,6,7,8-tetrahydrocadalene Simonellite	Trimethylnaphthalenes	
4-2	Anoxic	late Albian	Unknown 17β,21β(H)-hopane 17β,21β(H)-homohopane Trisnorisohop-13(18)-ene Hop-17(21)-ene Isohop-13(18)-ene 17β(H)-trisnorhopane	Δ^5-sterenes $C_{27} > C_{29}$ Δ^4-sterenes $C_{27} > C_{29}$ $\Delta^{5,22}$-steradienes C_{28} 5α,14α,17α(H)-steranes $C_{27} > C_{29}$ A monoaromatic steranes $C_{27} > C_{29}$	13-methylpodocarpa-8,11,13-triene Cadalene 19-norabieta-4,8,11,13-tetraene		
4-3	Anoxic	late Albian	Trisnorisohop-13(18)-ene Unknown Trisnorhop-17(21)-ene	Δ^5-sterenes $C_{27} \gg C_{29}$ Δ^4-sterens $C_{27} \gg C_{29}$ Diasterenes $C_{27} - C_{29}$ 5α,14α,17α(H)-steranes $C_{27} > C_{29}$ $\Delta^{5,22}$-steradienes C_{28}	Simonellite 13-methylpodocarpa-8,11,13-triene 19-norabieta-4,8,11,13-tetraene Abieta-7,13-diene Cadalene		
4-5	Anoxic	late Albian	Unknown Unknown Hop-17(21)-ene Isohop-13(18)-ene 17β,21β(H)-hopane 17β(H)-trisnorhopane 17β,21β(H)-homohopane 17α,21β(H)-hopane	5α,14α,17α(H)-steranes $C_{29} > C_{27}$ Δ^5-sterenes $C_{29} > C_{27}$ Δ^4-sterenes $C_{29} > C_{27}$ Diasterenes $C_{29} > C_{27}$ $\Delta^{5,22}$-steradienes C_{28} A monoaromatic steranes $C_{27} > C_{29}$	Not determined		
20-1	Anoxic	Jurassic (Pliensbachian/Sinemurian)	Trisnorhop-17(21)-ene Trisnorisohop-13(18)-ene Hop-17(21)-ene 17β-Trisnorhopane 17β,21β(H)-norhopane 17β,21β(H)-hopane 17β,21β(H)-homohopane 17α,21β(H)-hopane	A monoaromatic steranes $C_{27} > C_{29}$ 5α,14α,17α(H)-steranes $C_{27} > C_{29}$	Norsimonellite 13-methylpodocarpa-8,11,13-triene		
22-2	Oxic	Jurassic (Sinemurian)	17β,21β(H)-hopane 17β,21β(H)-homohopane 3-methyl-17α,21β(H)-hopane Unknown 17β,21α(H)-hopane 17β(H)-trisnorhopane 17β,21β(H)-norhopane	Under detectable level	Cadalene		
26-1	Oxic	Early Jurassic/late Triassic	17β,21β(H)-homohopane 17α,21β(H)-hopane 17α,18α,21β(H)-28,30-bisnorhopane 17β,21β(H)-hopane C_{37} homolog, unsaturated in side chain	Under detectable level	Not found		
Site 545							
29-1	Anoxic	late or middle Cenomanian	17β(H)-trisnorhopane Trisnorisophop-13(18)-ene 17β,21β(H)-hopane 17β,21β(H)-homohopane Isohop-13(18)-ene 17α,21β(H)-hopane	Diasterenes $C_{27} > C_{29}$ A monoaromatic steranes $C_{27} > C_{29}$	Cadalene 5,6,7,8-tetrahydrocadalene Dehydroabietane	Tetramethylnaphthalenes Trimethylnaphthalenes Dimethylnaphthalenes	
37-2	Anoxic	late Albian	17β,21β(H)-hopane 17β,21β(H)-homohopane Trisnorisohop-13(18)-ene Isohop-13(18)-ene 17β(H)-trisnorhopane 17α,21β(H)-hopane 17β,21β(H)-norhopane	A monoaromatic steranes $C_{27} > C_{29}$ Diasterenes C_{28} 5α,14α,17α(H)-steranes $C_{27} > C_{29}$ Δ^5-sterenes $C_{27} > C_{29}$ Δ^4-sterenes $C_{27} > C_{29}$ $\Delta^{5,22}$-steradienes C_{28}	13-methylpodocarpa-8,11,13-triene		
55-5	Anoxic	late Aptian	17β,21β(H)-homohopane 17β,21β(H)-hopane 17α,21β(H)-hopane 17β,21β(H)-norhopane Isohop-13(18)-ene	A monoaromatic steranes $C_{29} > C_{27}$ 5α,14α,17α(H)-steranes C_{27} Δ^5-sterenes C_{27} Δ^4-sterenes C_{27}	Cadalene Simonellite	Trimethylnaphthalenes Tetramethylnaphthalenes	

[a] Listed from more to less abundant.

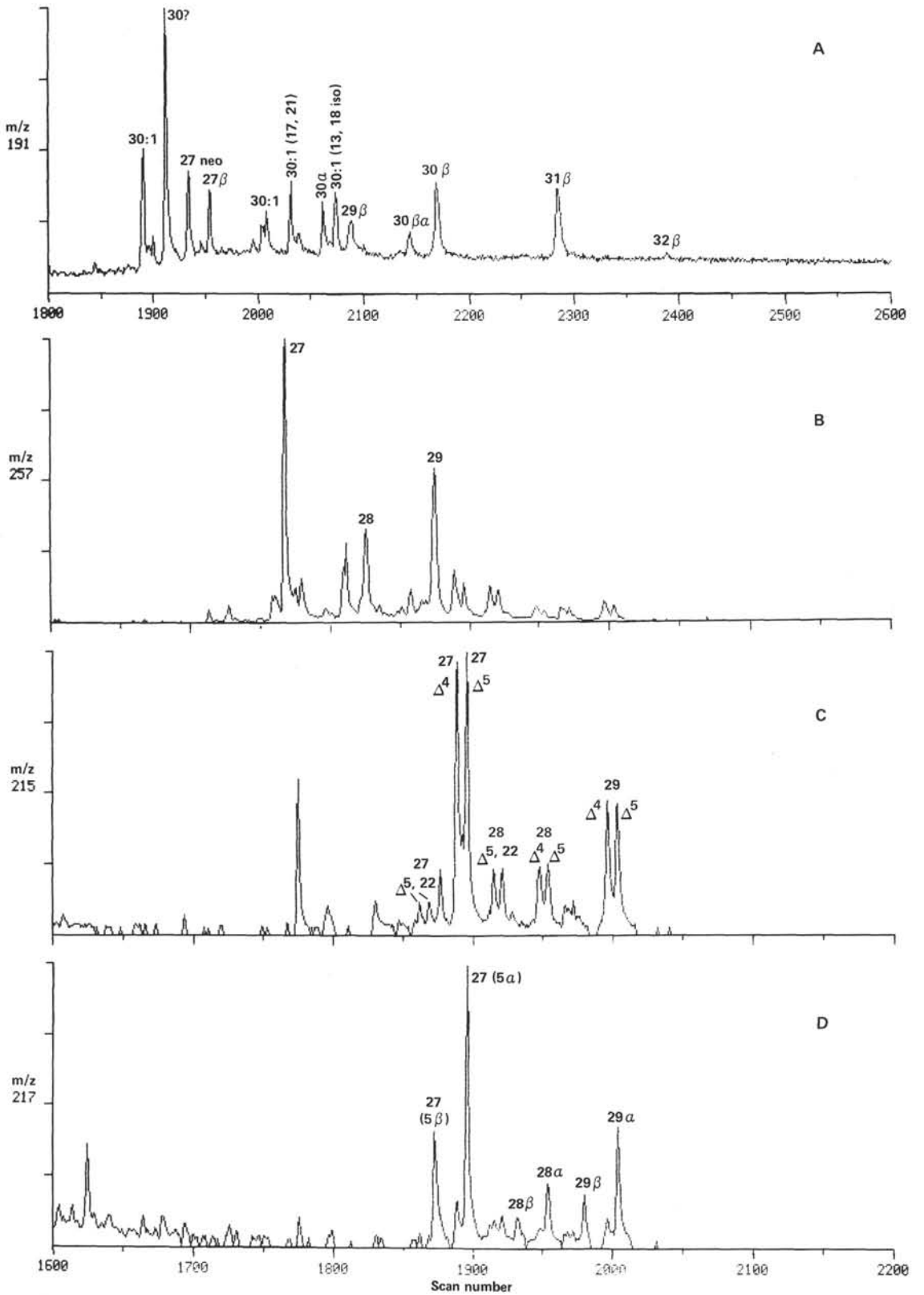

Figure 6. Salient features of the GC/MS data for an example of the hydrocarbon fraction from Albian Sample 547B-4-2, 110–126 cm. (Numerals indicate carbon numbers of compounds). A. Mass chromatogram m/z 191, triterpenoids. B. Mass chromatogram m/z 257, diasterenes. C. Mass chromatogram m/z 215, sterenes. D. Mass chromatogram m/z 217, steranes.

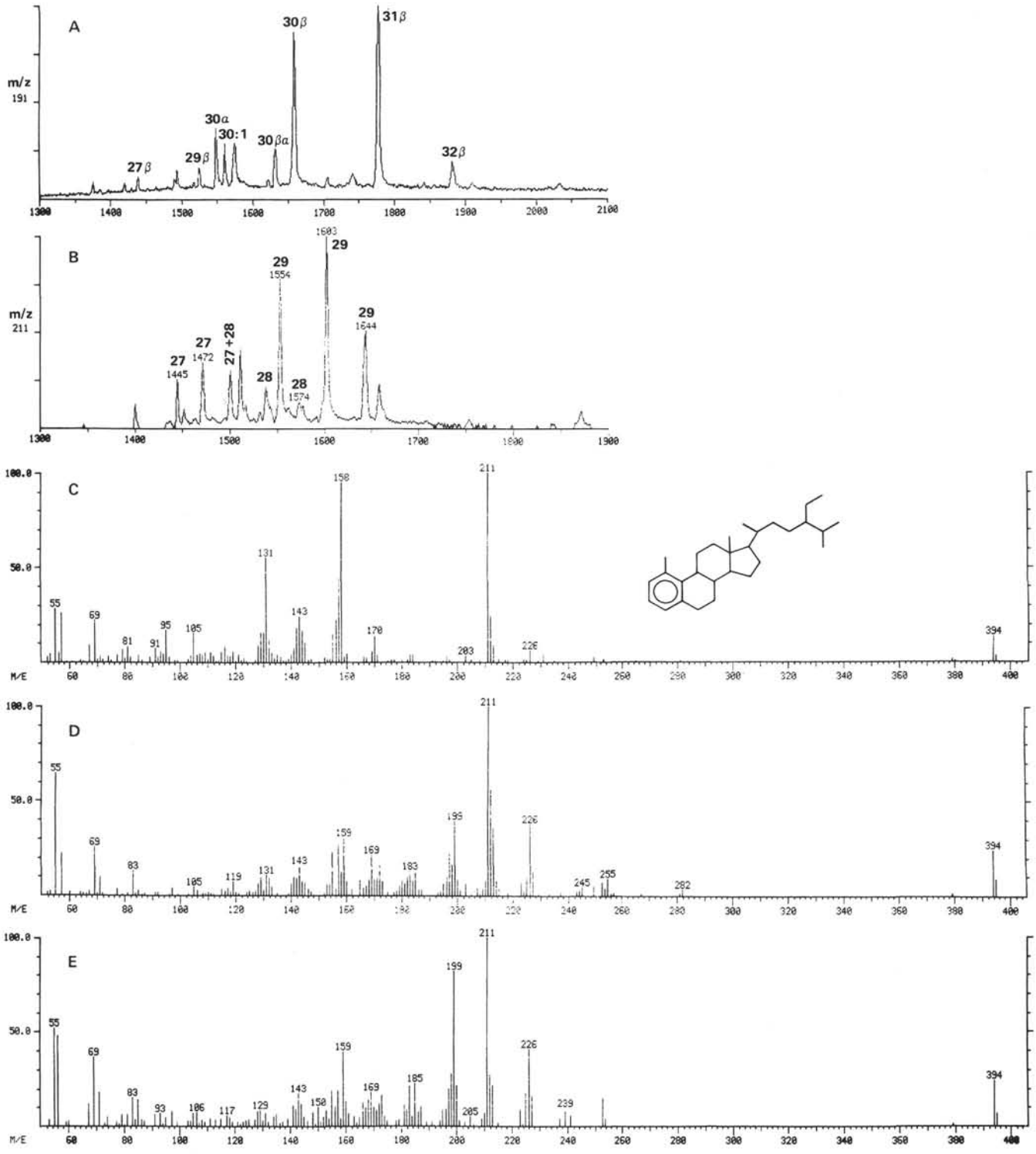

Figure 7. Salient features of the GC/MS data for the hydrocarbon fraction from Sample 545-55-5, 120–123 cm: A. Mass chromatogram m/z 191, triterpenoids. B. Mass chromatogram m/z 211, monoaromatic steranes, VIII. C. Mass spectrum, scan 1603 in Fig. 7B, 1-methyl-24-ethyl-19-norcholesta-1,3,5(10)-triene. D. Mass spectrum, scan 1554 in Fig. 7B, another C_{29}-isomer. E. Mass spectrum, scan 1644 in Fig. 7b, another C_{29}-isomer.

ries. Furthermore, the presence of the uncommon triterpenes, as, for example, isohopanes and fernenes, may indicate in the case of these samples some higher plant origin, since the paleoreconstruction of the depositional environments of both sites indicates rapid wash in of terrestrial detritus from wet zones (Simoneit and Stuermer, 1982). A terrigenous origin for some of the molecular markers is also supported by the dominant *n*-alkanes derived from vascular plant waxes and the Type III kerogens described later.

Rock-Eval Data and Organic Potentials of Sediments

The Rock-Eval data are given in Table 4 for samples from Site 547 and the results of the hydrogen index (HI) are plotted versus the oxygen index (OI) in Figure 8. There are three distinctive groups of samples based on their HI, namely, with high, moderate, and low values of HI, as is evident from the regions indicated on the Van Krevelen type diagram (Fig. 8). The conventional labels of the evolution paths are also indicated, but they should be considered as approximate trends. The first group consists of the organic-rich Jurassic and Tertiary samples and includes the I.F.P. standard 27251, which is a lower Toarcian organic-rich shale, an alginite and with an advanced path of kerogen evolution (Tissot et al., 1974; Espitalié et al., 1977). The second group includes all middle Cretaceous samples with moderate HI values, whereas the third group comprises all samples lean in C_{org} and derived from the youngest and oldest sediments cored. The same kind of grouping was observed for all sites of Leg 79 based on the on-board Rock-Eval measurements of many other samples (Site Chapters, this volume).

The T_{max} of all Cretaceous and Upper Jurassic samples ranges from 405 to 426°C. These low values, coupled with a negligible S1 peak (free hydrocarbons), indicate that these sediments are immature. This immaturity is supported further by the transformation ratio, S1/(S1 + S2) (Tissot and Welte, 1978), which is approximately zero for all samples. The hydrocarbon-generating potential, based on S2, ranges from poor to excellent.

The T_{max} of 509°C for the Pliocene sample (Unit I, Sample 547A-4-1, 110-116 cm), coupled with the high OI and low HI, indicate oxidized, mature, and probably recycled organic detritus. The low T_{max} (388°C) of the middle Miocene sample (Subunit IIA, Sample 547A-10-2, 120-136 cm) with the low HI and relatively high OI indicate oxidized but immature organic detritus. These inferences are also obvious from the plot of HI versus OI (Fig. 8), where these samples fall on the Type III kerogen path (vitrinitic).

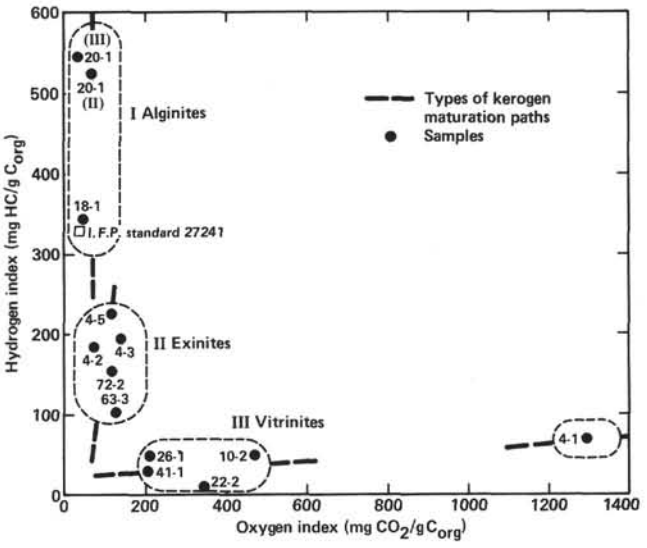

Figure 8. Rock-Eval data for the bulk organic matter plotted as hydrogen index versus oxygen index.

Sample 547A-18-1, 57–73 cm (Unit III, late Eocene) has an excellent hydrocarbon potential and the organic matter is an immature alginite (Type I kerogen). The Early Jurassic samples (Subunit VIB, Sample 547B-20-1, 5–23 cm, organic-rich vs. lean) also contain immature alginite organic matter (Type I kerogen) with only a relative concentration difference, probably due to mineral dilution of the organic detritus.

The late Cenomanian (Subunit VA, 547A-41-1, 34–50 cm); Early Jurassic (Subunit VIB, 547B-22-2, 36–55 cm); and the Jurassic/Triassic (Subunit VII, 547B-26-1, 20–36 cm) samples all fall on the Type III kerogen path (vitrinitic), have a very low hydrocarbon potential and elevated T_{max}, especially the Jurassic sample (503°C). These data indicate that the organic matter is probably derived from terrigenous sources, was partially oxidized during transport, and has also matured (mainly Sample 547B-22-2, 36–55 cm).

All samples from the late Albian (Subunit VB) cluster on the HI/OI plot (Fig. 8) and fall on both paths for

Table 4. Rock-Eval pyrolysis data for samples from Site 547.

Sample (interval in cm)	Sub-bottom depth (m)	Unit	Age	C_{org} (%)	S_1 (mg/g sediment)	S_2 (mg/g sediment)	S_3 (mg/g sediment)	Hydrogen index (HI) (mg HC/g C_{org})	Oxygen index (OI) (mg CO_2/g C_{org})	T_{max} (°C)
Hole 547A										
4-1, 110–116	99.5	I	Pleistocene/ Miocene	0.07	0.0	0.05	0.91	66	1297	509
10-2, 120–136	158.2	IIA	Miocene	0.19	0.0	0.09	0.89	47	470	388
18-1, 57–73	232.1	III	late Eocene	5.45	0.0	48.5	2.27	339	42	423
41-1, 34–50	440.9	VA	late Cenomanian	0.48	0.0	0.14	0.98	28	205	425
63-3, 110–126	553.6	VB	late Albian	0.93	0.0	0.96	1.17	103	126	420
72-2, 24–40	726.4	VB	late Albian	0.78	0.0	0.20	0.89	153	115	426
Hole 547B										
4-2, 110–126	755.7	VB	late Albian	1.16	0.0	2.11	0.85	182	74	423
4-3, 85–101	757.1	VB	late Albian	0.71	0.0	1.38	0.99	194	139	417
4-5, 10–26	759.5	VB	late Albian	0.88	0.0	1.97	1.02	224	116	417
$20^{(II)}$-1, 5–23	891.1	VID	Jurassic	2.02	0.0	10.6	1.27	526	63	408
$20^{(III)}$-1,5–23	891.1	VID	Jurassic	8.90	0.0	48.5	2.77	546	31	405
22-2, 36–55	907.0	VID	Jurassic	0.47	0.0	0.05	1.61	10	343	503
26-1, 20–36	941.7	VII	Jurassic/Triassic	0.28	0.0	0.14	0.58	49	209	450
(I.F.P. standard 27251)			lower Toarcian	2.48	0.0	8.2	0.85	330	34	426

Type I and Type II kerogens (alginites and exinites). The resolution of type I versus II is not possible from these data and would require microscopic maceral analysis. However, based on the meager hydrocarbon-generating potential (S2 range 0.1–2.1, Table 4), these samples appear to contain immature, degraded microbial detritus.

CONCLUSIONS

1. A strong terrestrial lipid input is observed for all the samples studied. In this respect, the corresponding *n*-alkane distributions have a dominant contribution of odd carbon number homologs $>n\text{-}C_{24}$, indicative of a higher plant wax origin. These profiles have different maxima (Fig. 5) depending on the location and age of the sections. Those from Site 545 (mid-Cretaceous) maximize at $n\text{-}C_{25}$, some from Site 547 (late Eocene to late Albian) at $n\text{-}C_{27}$, and others from Site 547 (Pleistocene to late Eocene and Jurassic) at $n\text{-}C_{31}$. The *n*-hydrocarbon distributions from Site 547 parallel those of Site 397 (located further to the south) and the predominance of $n\text{-}C_{31}$ in Jurassic sections has also been observed for the same age interval at Site 391 (Stuermer and Simoneit, 1978). This alternation between the maxima at $n\text{-}C_{31}$ to $n\text{-}C_{27}$ and again to $n\text{-}C_{31}$ may be due to terrestrial hydrocarbons coming from grassland or swamp vegetation in the first and third cases and from marsh or sea grasses in the second.

2. The autochthonous inputs are more evident for Site 545 where the *n*-alkanes exhibit a lower maximum at $n\text{-}C_{17}$ with essentially no carbon number preference from $n\text{-}C_{14}$ to $n\text{-}C_{20}$ (indicative of an algal origin). A marine origin may also be attributed to the major hump maximizing around $n\text{-}C_{17}$. In general these sections contain a relatively low concentration of *n*-alkanes below $n\text{-}C_{20}$, which may indicate strong microbial hydrocarbon degradation during deposition.

In some sections of Site 547 marine inputs are also evident. Thus, a maximum around $n\text{-}C_{21}$, attributable to algal/microbial products, is observed in Section 547A-18-1, and a high content of $n\text{-}C_{17}$ and $n\text{-}C_{19}$ in Section 547A-63-3 is indicative of bacterial detritus. On the other hand, Rock-Eval analyses of some samples of this site (Sections 547A-18-1, 547A-20-1) characterized their kerogens as alginites.

3. The oxicity or anoxicity of these sediments can be substantiated by means of two parameters: (a) the pristane and phytane concentrations (Didyk et al., 1978); and (b) the Rock-Eval indexes HI and OI (Tissot et al., 1974). In the first case, oxic samples (Sections 547A-4-1, 547A-10-2, 547A-41-1, 547B-22-2, and 547B-26-1) are distinguished by a higher amount of pristane over phytane and a very low content of both, whereas the anoxic sediments (Sections 547A-18-1, 547A-20-4, 547A-63-3, 547A-72-2, 547B-4-2, 547B-4-3, 547B-4-5, 547B-20-1) have a greater content of phytane than pristane at a higher overall concentration. With respect to the record parameter, there is a high OI and low HI for the oxic sections and a low OI with a high HI for the anoxic ones.

4. The degree of oxicity and the organic matter maturity generally correlate for Site 547. In this sense, the Rock-Eval analyses indicated that the sections from the mid-Cretaceous, Sections 547A-18-1 (Eocene) and 547B-20-1 (Jurassic), were immature (negligible S_1 peaks and low temperature maxima for hydrocarbon yield, T_{max}), and they could be classified either as alginites or exinites. Furthermore, the low amounts of normal hydrocarbons versus total organic carbon or their low yields may be related to their immaturity, which would support the presence of more polar material (carboxylic acids, ketones, etc.) in the bitumen.

With the exception of Section 547A-10-2 (Miocene), the oxic sections of Site 547 can be classified as mature due to their high T_{max} (509°C) and low hydrocarbon yield potential. In contrast, Section 547A-10-2 displays a low T_{max} (388°C) and the HI and OI are indicative of an oxidized but immature example. The unique *n*-alkane distribution and hump of the oldest sample (Section 547B-26-1, Triassic-Jurassic) can be explained in terms of geothermal processes, which would have caused its maturation and would have altered the original hydrocarbon profile with alkanes produced from the kerogen.

5. The molecular markers are mainly steroidal and triterpenoidal compounds. Samples from the mid-Cretaceous and late Eocene (Section 547A-18-1) have a higher amount of sterenes than hopanoids. Δ^4 and Δ^5-sterenes are the most common with a lower amount of steradienes ($\Delta^{5,22}$). C_{27} and C_{29} homologs are found in comparable amounts pointing to a mixed marine and terrestrial origin. C_{27} and C_{29} 5α(H)-steranes are also present. The hopanoid distribution ranges from C_{27} to C_{33} (no C_{28}) with a predominance of the $\beta\beta$ stereomers. Other unsaturated hopenes, trisnorhopenes, and fernenes are also found in these samples. Section 547B-20-1 (Early Jurassic) also contains the same kinds of compounds, with a predominance of the hopanoid over the steroid structures. Strong reducing paleoenvironmental conditions are indicated for these samples according to these molecular marker distributions (many unsaturated structures and the predominance of the $\beta\beta$ hopane series). The mid-Cretaceous samples of Site 545 contain ring A monoaromatized steroids (VIII) as major molecular markers, along with the same types of sterenes, steranes, steradienes, hopenes, and hopanes as those described previously. The presence of monoaromatized steranes has been reported for other Cretaceous black shales (Sites 364 and 365, Angola and Cape Verde basins, Hussler et al., (1981), which are also immature and from reductive paleoenvironments. These compounds were inferred to result from microbial and chemical transformation during early diagenesis; it is thus noteworthy that strong microbial activity was also observed for Site 545. The oxic samples contain no steroidal structures at the analytical level of detection and only minor amounts of saturated hopanoids. Nevertheless, it has to be pointed out that they are predominantly of the 17β(H), 21β(H) stereochemistry, even for the oldest sample (Section 547B-26-1, Jurassic–Triassic).

ACKNOWLEDGMENTS

We thank the National Science Foundation for access to the core samples by the direct participation of one of us (V.T.V.) aboard *Glo-*

mar Challenger as organic geochemist. We thank the Interdepartmental Commission for Research and Technological Investigation (CIRIT, Generalitat de Catalunya) for a research fellowship (J.O.G.); J. LeClaire and the shipboard technical staff for valuable assistance during sample collection and preliminary laboratory evaluations on Leg 79; Mrs. A. Vucheva, Geological Institute, Bulgarian Academy of Sciences, Sofia, for technical assistance while at O.S.U.; R. Mark Leckie (University of Colorado) for the determination of the foraminiferal assemblages; and Drs. P. A. Meyers and R. Cunningham for review of this manuscript.

REFERENCES

Didyk, B. M., Simoneit, B. R. T., Brassell, S. C., and Eglinton, G., 1978. Organic geochemical indicators of paleoenvironmental conditions of sedimentation. *Nature*, 272:216–222.

Espitalié, J., LaPorte, J. L., Madec, M., Marquis, F., LePlat, P., Paulet, J., and Boutefeu, A., 1977. Methode rapide de caractérisation des roches mères de leur potentiel pétrolier et de leur degré d'evolution. *Rev. Inst. Fr. Pet*, 32:23–42.

Giger, W., Schaffner, C., and Wakeham, S. G., 1980. Aliphatic and olefinic hydrocarbons in recent sediments of Greifensee, Switzerland. *Geochim. Cosmochim. Acta*, 44:119–129.

Hinz, K., Dostmann, H., and Fritsch, J., 1982. The continental margin at Morocco: seismic sequences, structural elements and geological development. *In* von Rad, U., Hinz, K., Sarnthein, M., and Seibold, E. (Eds.), *Geology of the Northwest African Continental Margin*: Berlin (Springer), pp. 34–60.

Huang, W. Y., and Meinschein, W. G., 1979. Sterols as ecological indicators. *Geochim. Cosmochim. Acta*, 43:739-745.

Hussler, G., Chappe, B., Wehrung, P., and Albrecht, P., 1981. C_{27}-C_{29} ring A monoaromatic steroids in Cretaceous black shales. *Nature*, 294:556–558.

Peters, K. E., and Simoneit, B. R. T., 1982. Rock-Eval pyrolysis of Quaternary sediments from Leg 64, Sites 479 and 480, Gulf of California. *In* Curray, J. R., Moore, D. G., et al., *Init. Repts DSDP*, 64, Pt 2: Washington (U.S. Govt. Printing Office), 925–931.

Reed, W. E., 1977. Molecular compositions of weathered petroleum and comparison with its possible source. *Geochim. Cosmochim. Acta*, 41:237–247.

Roucaché, J., Deroo, G., and Boulet, R., 1979. Caractérization par differentes méthodes physicochimiques des types de matière organique dans les sédiments du Cretacé d'Atlantique en mèr profonde. *Rev. Inst. Fr. Pet.* 34:191–220.

Rullkötter, J., Cornford, C., and Welte, D., 1982. Geochemistry and petrography of organic matter in Northwest African continental margin sediments: quantity, provenance, depositional environment, and temperature history. In Von Rad, U., Hinz, K., Sarnthein, M., and Seibold, E. (Eds.), *Geology of the Northwest African Continental Margin*: Berlin (Springer), pp. 686–703.

Simoneit, B. R. T., 1977. Diterpenoid compounds and other lipids in deep-sea sediments and their geochemical significance. *Geochim. Cosmochim. Acta*, 41:463–476.

_____, 1978. The organic chemistry of marine sediments. In Riley, J. P., and Chester, R., (Eds.), *Chemical Oceanography*: London, (Academic Press), pp. 233–311.

_____, 1982. Shipboard organic geochemistry and safety monitoring, Leg 64, Gulf of California. In Curray, J. R., Moore, D. G., et al., *Init. Repts DSDP*, 64, Pt. 2: Washington (U.S. Govt Printing Office), 723–727.

_____, in press. Cyclic terpenoids of the geosphere. In Johns, R. B. (Ed.), *Biological Markers, IGCP Mono.* 157: (Elsevier) Amsterdam.

Simoneit, B. R. T., and Mazurek, M. A. 1979a. Lipid geochemistry of Cretaceous sediments from Vigo Seamount, DSDP/IROD Leg 47B. *In* Sibuet, J. C., Ryan, W. B. F., et al., *Init. Repts. DSDP*, 47, Pt. 2: Washington (U.S. Govt Printing Office), 565–570.

_____, 1979b. Search for eolian lipids in the Pleistocene off Cape Bojador and lipid geochemistry of a Cretaceous mudstone, DSDP/IPOD Leg 47A. *In* von Rad, U., Ryan, W. B. F., et al., *Init. Repts. DSDP*, 47, Pt 1: Washington (U.S. Govt. Printing Office), 541–545.

Simoneit, B. R. T., and Stuermer, D. H. 1982. Organic geochemical indicators for sources of organic matter and paleoenvironmental conditions in Cretaceous oceans. *In* Schlanger, S. O., and Cita, M. B., (Eds.), *Nature and Origin of Cretaceous Carbon-rich Facies* London (Academic Press), pp. 145–163.

Spyckerelle, C., 1975. Constituants aromatiques de sediments (thèse). Universite Louis Pasteur, Strasbourg, France.

Stuermer, D. H., and Simoneit, B. R. T., 1978. Varying sources for the lipids and humic substances at Site 391, Blake-Bahama Basin, DSDP Leg 44. *In* Benson, W. E., Sheridan, R. E., et al., *Init. Repts. DSDP*, 44: Washington (U.S. Govt. Printing Office) 587–591.

Tissot, B., Durand, B., Espitalié, J., and Combaz, A., 1974. Influence of nature and diagenesis of organic matter in formation of petroleum. *Am. Assoc. Pet. Geol. Bull.*, 58:499–506.

Tissot, B. P., and Welte, D. H., 1978. *Petroleum Formation and Occurrence: A New Approach to Oil and Gas Exploration*: Berlin, (Springer-Verlag).

Vuchev. V. T., 1974. Studies of organic matter in the Triassic carbonates of northern Bulgaria. *In* Tissot, B., and Bienner, F. (Eds.), *Advances in Organic Geochemistry 1973*, Paris (Editions Technip), pp. 489–505.

Wakeham, S. G., and Carpenter, R., 1976. Aliphatic hydrocarbons in sediments of Lake Washington. *Limnol. Oceanogr.*, 21:711–723.

Date of Initial Receipt: August 9, 1983
Date of Acceptance: October 28, 1983

APPENDIX
Chemical Structures Cited in the Text

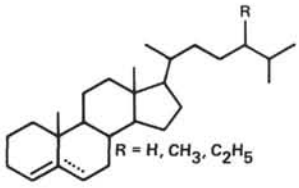

I. Δ^4- or Δ^5- Sterenes

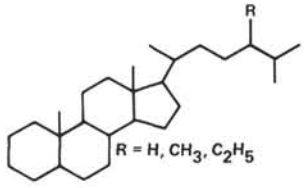

II. 5α (H)- Steranes

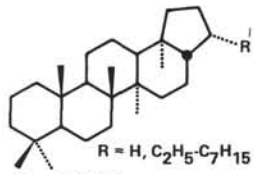

III. 17β (H)-Hopanes

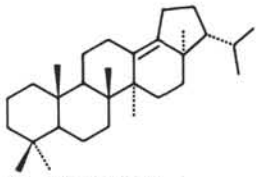

IV. Isohop-13(18)-ene

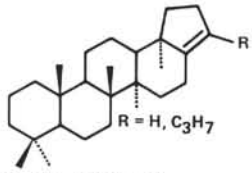

V. Hop-17(21)-enes

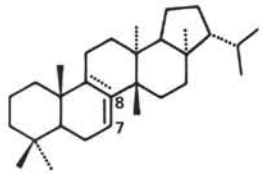

VI. Fernenes

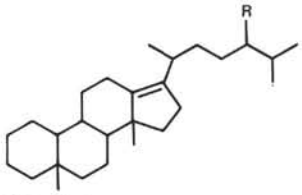

VII. Diasterenes

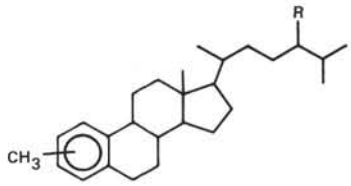

VIII. Monoaromatic steranes

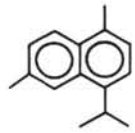

IX. Cadalene

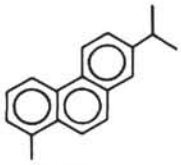

X. Retene

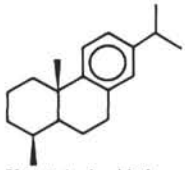

XI. Dehydroabietin

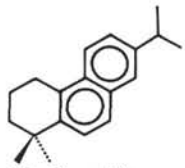

XII. Simonellite

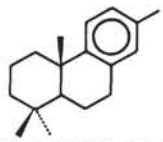

XIII. 13-Methylpodocarpa-8, 11-13-triene